The crystal length modulation for the entangled biphotons generated by SPDC

J. B. WANG[1,2], H. B. LIN[2,*]
[1]*College of Mechanical Engineering, Zhejiang University of Technology, Hangzhou 310014, China*
[2]*Institute of Mechanical & Electrical Technology, Taizhou Vocational & Technical College, Taizhou 318000, China*

We demonstrate the quantum entanglement of the entangled biphotons generated by type II spontaneous parametric down-conversion(SPDC) through a nonlinear crystal with phase-matching conditions. We find that the shorter crystal length, makes the main mode be more obvious in the discrete Schmidt modes, and also the corresponding eigenvalues, Weight, and Schmidt Numbers. Hence, shortening of the length of the crystal can further simplify the selection of modes, slightly increase the frequency response range of the down-conversion process, and compress the temporal width of the pulse. Our research is helpful to generate the ultrashort entanglement biphotons in nonlinear optics.

(Received September 21, 2023; accepted April 10, 2024)

Keywords: Biphotons, SPDC, Entanglement

1. Introduction

Quantum entanglement is a core physical concept in quantum mechanics, which is unique in the nonclassical physics. It plays a fundamental and important role in quantum optics, and it has a wide range applications in quantum teleportation [1,2], quantum cryptography[3] and other related aspects.

There are many methods to generate entanglement, and one of the easiest and most effective methods is the entangled biphotons generated by spontaneous parametric down conversion(SPDC) process. In this process, the pump light (with frequency ω_p) is incident into a nonlinear crystal, and split into two lower frequency photons named as signal photon(with frequency ω_s) and idler photon(with frequency ω_i). This process is promoted by the second-order nonlinear effect which is caused by the interaction between the pump light and the nonlinear crystal [4]. These two photons are spontaneously and simultaneously generated with a high degree of correlation and entanglement [5,6]. The degree of entanglement can be effectively improved when energy conservation or momentum conservation is satisfied between the pump, signal and idler photons involved in SPDC [7]. These entanglements show many degrees of freedom, including spatial, frequency and polarization [8-13]. These are tunable entangled physical quantities in the spectral and time domains, such as wave vectors, transverse and orbital angular momentum entanglements [11,14,15]. They can be modulated as Hilbert space degrees of freedom. When a certain quantity is chosen to distinguish the biphoton system, another physical quantity can describe the corresponding biphoton state [7,16,17]. Among the various degrees of freedom for entanglements, polarization is a relatively simple one, which is conducive to a more profound understanding of the properties of entanglement. The entanglement of biphotons can be described and investigated by the two-dimensional Hilbert space in the direction of polarization generated by SPDC. It also includes defining and modulating entropy [9,18]. Meanwhile, the Schmidt decomposition enables further exploration entanglement of the spectral, correlation and other properties of the biphotons generated with multimode compression, and it is also an important theoretical analytical tool for multimode entanglement. The entanglement of biphotons generated by SPDC is closely related to the type of the down conversion, the crystal length, the pump envelope function, and other related parameters in a higher-dimensional system [10,19-22].

In general, the spectral response frequency range would be broadened and the entanglement would be enhanced as the crystal length decreases. In order to further verify the validity of these conclusions, we explore the influence of crystal length on the properties of Schmidt modes and entanglement involved in the process of SPDC in nonlinear crystals.

In this paper, we mainly discuss how the polarization entanglement of biphotons generated by SPDC is affected by the crystal length, and how the effective modulation of entanglement can be achieved by the crystal length. Meanwhile, we analyze the Schmidt modes in discrete modes by the Schmidt decomposition according to the Ref.10 and discuss the distribution of eigenvalues and entropy, specifically discussing the modulation effect of the crystal length on the eigenvalues.

2. Theory for Schmidt decomposition

In the SPDC, the pump light incidents into the crystal and splits into two lower frequency entangled photons, and the state function can be generally expressed as follows [23,24]:

$$|bi\rangle = \int F(\omega_s,\omega_i) a_s^{\dagger}(\omega_s) a_i^{\dagger}(\omega_i)|0\rangle_s|0\rangle_i d\omega_s d\omega_i \quad (1)$$

where $a_\mu^{\dagger}$ and a_μ are the creation and annihilation operators. $|0\rangle_\mu$ are the vacuum state for the signal and idler photons. μ represents the signal and idler photons. $F(\omega_s,\omega_i)$ is the joint spectral amplitude function with the signal frequency ω_s and idler frequency ω_i. This function represents the interaction between the three-mixed waves and the nonlinear crystal. It can be expressed as the product of the pump envelope function $\chi(\omega_s,\omega_i)$ and the phase-matching function $\phi(\omega_s,\omega_i)$:

$$F(\omega_s,\omega_i) = \eta\chi(\omega_s,\omega_i)\phi(\omega_s,\omega_i) \quad (2)$$

where η is a normalized constant to satisfy the normalization condition $\int|F(\omega_s,\omega_i)|^2 d\omega_s d\omega_i = 1|$. The pump envelope function can be a Gaussian which expressed as follows:

$$\chi(\omega_s,\omega_i) \sim exp\left[-\frac{(\omega_s+\omega_i-\omega_p)^2}{2\sigma_p^2}\right] \quad (3)$$

Δk is the wave-vector mismatching for the three mixed waves in the crystal. σ is the bandwidth of pump photon. The phase matching function $\phi(\omega_s,\omega_i)$ for the nonlinear crystal can make the three-mixed waves and the crystal phase matched. And in this paper it can be expressed as a sinc function for the phase matching [10].

$$\phi(\omega_s,\omega_i) = sinc\left[\frac{\Delta k(\omega_s,\omega_i)L}{2}\right] \quad (4)$$

The phase matching function is associated with phase mismatching Δk and the crystal length L. Especially, the Δk shows the relationship for the wave vectors among the three waves and satisfies the relationship as follows:

$$\Delta k = k_p - k_s - k_i \simeq \sum_\mu(\omega_\mu-\omega_0)(k'_p - k'_\mu) \quad (5)$$

where k'_μ denotes the reciprocal of the group velocity for the signal or the idler photon. This equation is the exact representation and first order approximation of the phase matching function. In this paper, with the help of Schmidt decomposition, the continuous spectrum for the biphotons can be discretized into the discrete modes according to the method in Ref.[10,25]. After converting the continuous spectrum of biphotons, it is more convenient to analyze the structure, eigenvalues and entropy distributions of their discrete modes, and to discuss the modulation effect of the crystal length on the discrete entanglement of the biphotons during the SPDC.

As expressed by Eq.(1), if the two photons are independent without any frequency correlation, the joint spectral amplitude function $F(\omega_s,\omega_i)$ is factorizable and the biphotons state has no entanglement in frequency domain for the reason that there is no one-to-one relation between the signal and idler frequency. When the joint spectral amplitude function cannot be factorized in the form of ω_s and ω_i, we can say that the biphotons state $|bi\rangle$ is entangled in the frequency domain[10]. The correlation between the signal and idler photons can be expressed by the joint spectral amplitude function, whose square modulus represents the probability. And this function is determined by the interaction between the three mixed waves and the nonlinear crystal.

In order to further explore the entanglement properties between them, the continuous modes in Eq.(1) can be transformed by discrete modes by Schmidt decomposition. When the joint spectral amplitude function $\mathrm{F}(\omega_s,\omega_i)$ in Eq.(1) cannot be factorized into the product of ω_s and ω_i, it implies that there is entanglement between the two photons[10,26]. Hence, the joint spectral amplitude function $\mathrm{F}(\omega_s,\omega_i)$ can be decomposed by Schmidt decomposition and the corresponding eigenbasis is obtained as follows:

$$\mathrm{F}(\omega_s,\omega_i)=\sum_{n=1}^{\infty}\sqrt{\lambda_n}u_n(\omega_s)v_n(\omega_i) \tag{6}$$

where $\sqrt{\lambda_n}$ is the eigenvalue of the eigenfunction, $\mathrm{n}=1,2,\ldots$ are the positive integer and satisfy the normalization condition. Orthogonal functions $u_n(\omega_s)$ and $v_n(\omega_i)$ are conjugate Schmidt modes. They are the eigenfunctions for the integral equations shown as follows [10,27]:

$$\int F(\omega_1,\omega_2)v_n^*(\omega_2)d\omega_2=\sqrt{\lambda_n}u_n(\omega_1) \tag{7}$$

$$\int u_n^*(\omega_1)F(\omega_1,\omega_2)d\omega_1=\sqrt{\lambda_n}v_n(\omega_2) \tag{8}$$

Or written as:

$$\iint F(\omega,\omega_1)F^*(\omega',\omega_1)v_n(\omega')d\omega_1 d\omega'=\int \rho_1(\omega,\omega')u_n(\omega')d\omega' \tag{9}$$

$$\iint F(\omega_2,\omega)F^*(\omega_2,\omega')u_n(\omega')d\omega_2 d\omega'=\int \rho_2(\omega,\omega')v_n(\omega')d\omega' \tag{10}$$

where ρ_1 and ρ_2 are the kernels for the one photon spectral correlations, and they satisfy $\rho_1(\omega,\omega')=\int F(\omega,\omega_2)F^*(\omega',\omega_2)d\omega_2$, $\rho_2(\omega,\omega')=\int F(\omega_1,\omega)F^*(\omega_1,\omega')d\omega_1$. u_n and v_n can be viewed as the eignenfunctions for these kernels:

$$\int \rho_1(\omega,\omega')u_n(\omega')\,d\omega'=\lambda_n u_n(\omega) \tag{11}$$

$$\int \rho_2(\omega,\omega')v_n(\omega')d\omega'=\lambda_n v_n(\omega) \tag{12}$$

The two eigenfunctions satisfies orthogonality relation:

$$\int u_m^*(\omega_1)v_n(\omega_1)d\omega_1=\delta_{m,n} \tag{13}$$

Eqs.(7) and (11) both define the Schmidt modes from different perspectives, and they are almost equivalent to each other. The only difference is that the phase of the Schmidt modes cannot be controlled by the reduced density matrix, and it is necessary to incorporate the corresponding arbitrary phase factor $\exp(i\vartheta_{uv})$ to satisfy the relational equation of Eq.(11). Phase modulation is performed according to θ, where the simplest case is to take $\theta=0$ and $\theta=\pi$ to denote the symmetric and antisymmetric cases, but Eq.(7) is not invariant with the addition of an arbitrary phase factor, and therefore when Eq.(7) is chosen to define the Schmidt modes, their phase factors are determined[27].

For individual non-zero eigenvalues, this means that there is entanglement between their corresponding Schmidt modes. For modes that are entangled with each other, when one of them is detected with a certain probability, the other will also be detected with a certain probability and satisfy the eigenvalue $\sum\lambda_n=1$.

The Schmidt decomposition is a good method for entanglement determination and provides the corresponding distribution of Schmidt mode particles, which also implies that in the pure state, the biphotons state can be detected correspondingly by pairing the Schmidt modes, while at the same time, for the same n, another particle under its conjugate mode v_n can be detected with a certain probability, and therefore the probability of detecting the corresponding entangled biphotons state in the mode $\{u_n,v_n\}$ is determined by the corresponding eigenvalue λ_n.

3. Results and discussions

We selected the parameters as shown in Ref.[10], and obtain the joint spectral intensity as shown in Fig. 1. The crystal lengths in Fig. 1(a) and (b) are $\mathrm{L}=0.001\mathrm{m}$ and $\mathrm{L}=0.002\mathrm{m}$, respectively. And the corresponding spectral power distributions have stronger spectral correlations when $\mathrm{L}=0.001\mathrm{m}$. As the crystal length increases, the strength of the spectral correlation gradually decreases. The shorter of the crystal length, the wider of the spectral frequency response range with the phase-matching condition, which matches the expectation that the width of the spectral response frequency is inversely proportional to the crystal length.

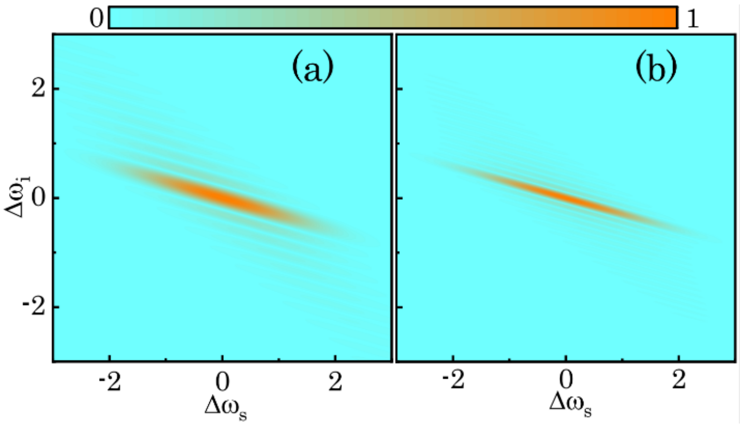

Fig. 1. Spectral power distributions for nonlinear crystal with lengths $L =$ (a).0.001 m and (b).0.002 m. The $\Delta\omega_{s,i}$ in the horizontal and vertical coordinates denote $\omega_{s,i} - \omega_0$ and are in σ, respectively. The shorter the crystal length, the stronger the corresponding spectral amplitude and wider the frequency response range (color online)

According to the eigenfunctions in continuous modes, they can be calculated by numerical simulation of the factorizable discrete matrices, and the eigenstates and the eigenvalues, can be obtained by Schmidt decomposition. When the joint spectral amplitude function is decomposed by Schmidt decomposition, the corresponding Schmidt modes are similar to that of a resonator. The number of wave peaks will increase and oscillates will be more violently with the increase of the mode n.

Especially when the crystal $\mathrm{L} = 0.002\mathrm{m}$, the oscillation of its boundary is more intense. Meanwhile, when the correlation of the spectral power in Fig.1 is compressed, the waveforms distribution of the corresponding modes is compressed, which also makes the peaks of their waveform distributions become larger in the same mode. When focusing on the $\mathrm{n} = 1,2,3$ modes, the corresponding Schmidt modes are shown in Fig.2. And they are similar to the modes of the resonator [10], which have a similar structure when we perform the Fourier transform on each of them to obtain the distributions in the time domain, and the oscillations of the modes are intensified as the number of modes increases. In this figure, it can be found by comparison that for the same n, the distribution of u_n and v_n mode has similarity, but not completely symmetric, the main reason is that this is a type II parametric conversion, the asymmetric phase matching function determines the distribution of modes cannot be realized completely symmetric as well.

In order to compare the phase distributions of each mode, we select the eigenvalue distributions for different crystal lengths as shown in Fig.3(a). It can be found that $\mathrm{n} = 1$ accounts for a larger proportion of all $\sqrt{\lambda_n}$ when the crystal length is shorter. As a result, the phase matching is much better at this crystal length, resulting in a greater concentration of multiple modes in the $\mathrm{n} = 1$ mode, which therefore has a much higher probability than the other modes. The shorter of the crystal length L, the higher value of the state occupied by the eigenvalues of the first few of them, i.e. the higher degree of entanglement and the state vector can be represented efficiently in a space with lower dimensions.

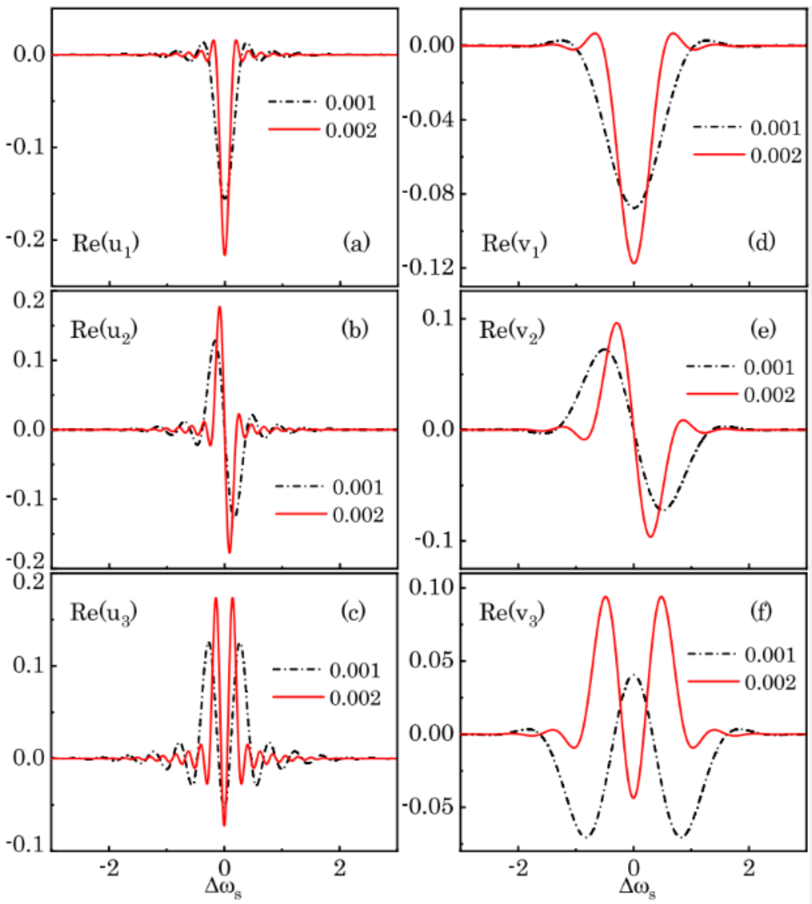

Fig. 2. The distribution of the modes of the Schmidt modes at the main (taking $n = 1,2,3$*) obtained by the Schmidt decomposition is also the distribution of the Schmidt states of the frequency-domain content in Fig. 1 (color online)*

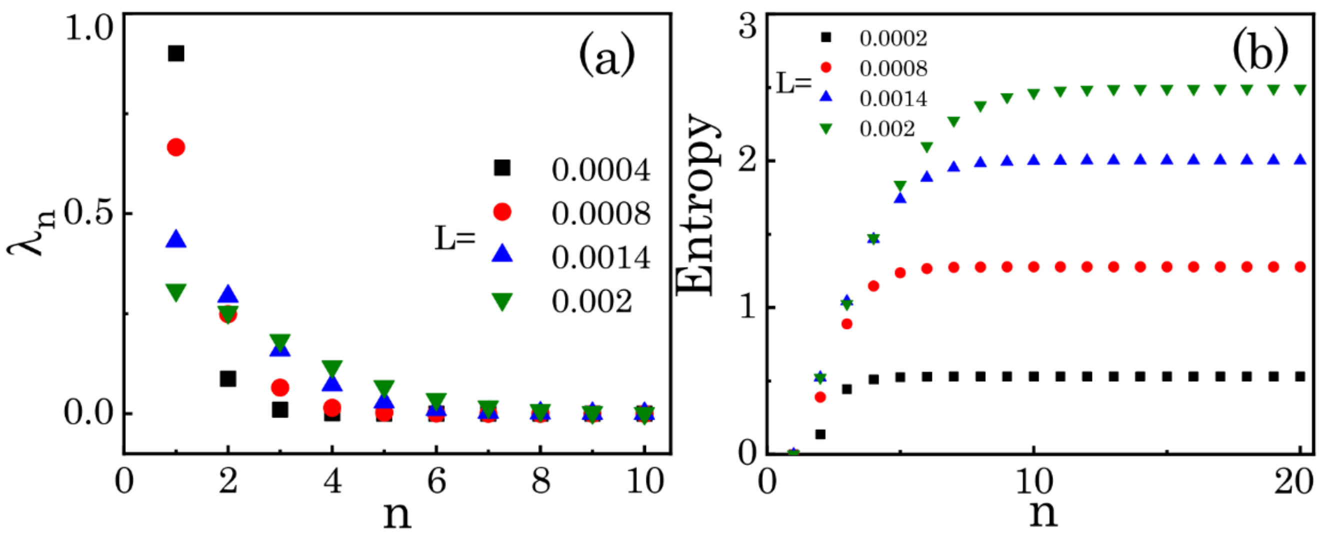

Fig. 3. Distribution of eigenvalues λ_n *and corresponding entropies obtained after Schmidt decomposition at different lengths of nonlinear crystals (color online)*

Similarly, according to the definition in Ref.[10], the probability distribution in each mode can be transformed into the distribution of the corresponding entropy.

The entanglement entropy can be defined as:

$$S_E = -\sum_{k=1}^{n} \lambda_k log_2 \lambda_k \tag{14}$$

As the crystal length increases, the probability distributions of the individual modes tend to stabilize, which results in a larger entropy value. As shown in Fig.3(b), the change of the front entropy is more drastic when the crystal length L is small. As n increases, the entropy values in different cases stabilize. But for the same n, a longer crystal length increases the entropy value, which is also due to the effect of phase matching. According to the distribution of eigenvalues converges to 0 when $n \to \infty$, so the entanglement entropy also converges to a specific value when $n \to \infty$, and the speed of convergence as well as the size of the convergence value is closely related to the distribution of the first few eigenvalues. The shorter of the crystal length L, the slower its entropy increases, corresponding to the proportion contributed under the first few eigenvalues, but in any case the convergence of the eigenvalues and entanglement entropy is satisfied in such cases. In order to facilitate the discussion, we concentrate calculate them in the spatial modes of lower dimensions.

On the basis of the above discussion, we introduce the weight function[23]:

$$\Lambda_n = \frac{[sinh(G\sqrt{\lambda_n})]^2}{\sum_n [sinh(G\sqrt{\lambda_n})]^2} \tag{15}$$

where G is parametric gain. And based on this, we obtain the corresponding value of K[21,23,28,29]:

$$\mathrm{K} = \frac{1}{\sum_n \Lambda_n^2} \tag{16}$$

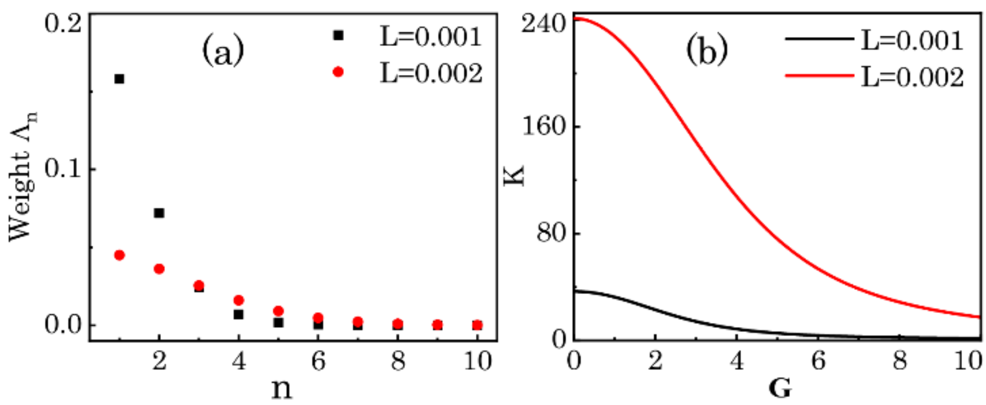

Fig. 4. Schmidt eigenvalues for nonlinear crystal lengths $L = 0.001m$ and $L = 0.002m$ of (a) Weight with G=1 and (b) Schmidt number K versus parametric gain G (color online)

It represents an estimate of the overall distribution of the eigenvalues obtained from the spatial model and can also be used to represent the average of the effective dimensions of the system. As shown in Fig.4 (a), for $L = 0.001m$, the Weight is more proportionally larger for smaller n such as $n = 1,2$. We can focus on the first 2 modes because they have higher probabilities. For the case of the first mode $n = 1$, the proportion occupied at $n = 1$ is particularly prominent when the crystal length is shorter, and the Weight is more stable with increasing n. As the crystal length increases, the probability distribution of each mode is flatter, which is also indicated by the K value distribution in Fig.4(b).

According to the characteristics of the Schmidt eigenvalue λ_n, since the eigenvalue in $n = 1$ is largest, i.e., the probability of the corresponding mode is highest in each mode. Therefore, we concentrate on $n = 1$ mode. Based on the characteristics of the frequency domain distribution in this mode, we convert it into a time domain distribution by the Fourier transformation:

$$U_n(t) \sim \int u_n(\omega) e^{i\omega t} d\omega \tag{17}$$

Although, a pulse with a broad frequency bandwidth does not necessarily lead to a narrow temporal width. It can be theoretically predicted that the shorter temporal width pulse can be obtained in the shorter crystal length due to the Fourier transformation with wider frequency band. By comparison in Fig.5, it can be found that the temporal width is well compressed when the crystal length $\mathrm{L} = 0.001\mathrm{m}$, and the full width at half maxima(FWHM) is compressed from 0.332 ps when $\mathrm{L} = 0.002\mathrm{m}$ to 0.174 ps when $\mathrm{L} = 0.001\mathrm{m}$. The temporal width is compressed nearly at a half, which is a good compression effect. Similarly, for the temporal distribution plot at $\mathrm{n} = 2$, as shown in Fig. 5(b), also the pulse width is narrower when the crystal $\mathrm{L} = 0.001\mathrm{m}$, and its compression effect can be applied to the case of a double-peak pulse[30].

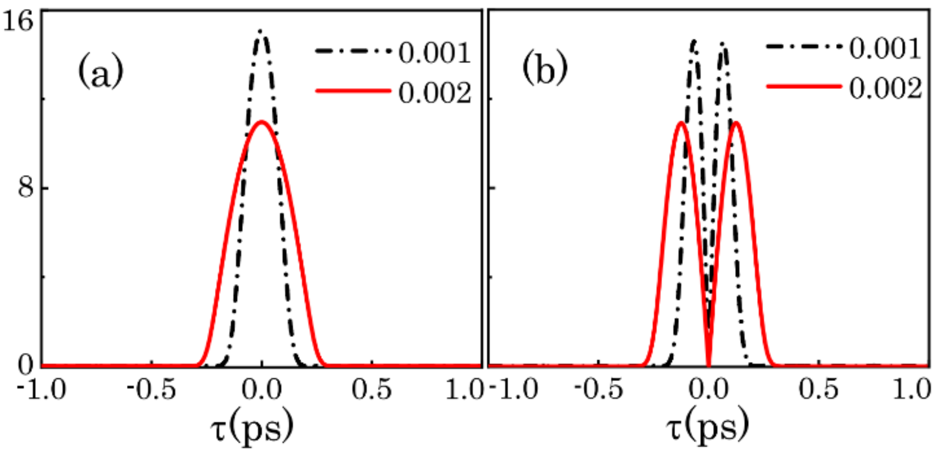

Fig. 5. Time-domain distributions of Schmidt modes for (a) $n = 1$ and (b) $n = 2$ with the nonlinear crystal lengths $L = 0.001m$ and $L = 0.002m$ (color online)

4. Conclusion

We demonstrate the modulation effect of the crystal length on quantum entanglement of the entangled biphotons generated by SPDC through a nonlinear crystal with phase-matching conditions. In particular, the conversion of a continuous integral function into a pair of discrete finite modes is discussed, which can detect the characteristics of the entanglement more accurately. Through the numerical analysis we find that the shorter of the crystal length, the more obvious the role of the main mode in the discrete Schmidt modes, and the more dominant of the corresponding eigenvalues, Weight, and Schmidt Numbers. Hence, shortening of the length of the crystal can further simplify the selection of modes, slightly increase the frequency response range of the down-conversion process, and compress the temporal width of the pulses with the Fourier transformation. We hope our research will contribute to pulse compression with high entanglement.

Acknowledgements

This work was supported by General scientific research project of Zhejiang Provincial Department of Education (Grant No. Y202250327), Taizhou Science and Technology Project (Grant No. 22gyb17), and Taizhou High-level Talent Special Support Program (2019, 2020).

References

[1] C. H. Bennett, G. Brassard, C. Crepeau, R. Jozsa, A. Peres, W. K. Wootters, Phys. Rev. Lett. **70**, 1895 (1993).
[2] D. Bouwmeester, J. W. Pan, K. Mattle, M. Eibl, H. Weinfurter, A. Zeilinger, Nature **390**, 575 (1997).
[3] A. K. Ekert, Phys. Rev. Lett. **67**(6), 661 (1991).
[4] J. P. Torres, K. Banaszek, I. A. Walmsley, Prog. Opt. **56**, 227 (2011).
[5] H. E. Brandt, Prog. Quantum Electron. **22**, 257 (1998).

[6] S. E. Harris, Phys. Rev. Lett. **98**(6), 063602 (2007).

[7] M. F. Saleh, B. E. A. Saleh, M. C. Teich, Phys. Rev. A **79**(5), 053842(2009)

[8] D. N. Klyshko, Photons and Nonlinear Optics, Nauka, Moscow, Ch. 1 and 6, 1980.

[9] P. G. Kwiat, K. Mattle, H. Weinfurter, A. Zeilinger, A. V. Sergienko, Y. Shih, Phys. Rev. Lett. **75**(24), 4337 (1995).

[10] C. K. Law, I. A. Walmsley, J. H. Eberly, Phys. Rev. Lett. **84**(23), 5304 (2000).

[11] A. Mair, A. Vaziri, G. Weihs, A. Zeilinger, Nature **412**, 313 (2001).

[13] J. T. Barreiro, N. K. Langford, N. A. Peters, P. G. Kwiat, Phys. Rev. Lett. **95**(26), 260501 (2005).

[14] E. Nagali, F. Sciarrino, F. De Martini, L. Marrucci, B. Piccirillo,E. Karimi, E. Santamato, Phys. Rev. Lett. **103**(1), 013601 (2009).

[15] A. Joobeur, B. E. A. Saleh, M. C. Teich, Phys. Rev. A **50**(4), R3349 (1994).

[16] A. Joobeur, B. E. A. Saleh, T. S. Larchuk, M. C. Teich, Phys. Rev. A **53**(6), 4360 (1996).

[17] D. B. Horoshko, M. I. Kolobov, Phys. Rev. A **88**(3), 033806 (2013).

[18] D. B. Horoshko, M. I. Kolobov, Phys. Rev. A. **95**(3), 033837 (2017).

[19] P. G. Kwiat, J. Mod. Opt. **44**, 2173 (1997).

[20] A. Christ, K. Laiho, A. Eckstein, K. N. Cassemiro, C. Silberhorn, New Journal of Physics **13**, 033027 (2011).

[21] X. Sanchez-Lozano, J. L. Lucio M., International Journal of Quantum Information **13**(5), 1550032 (2015).

[22] J. Svozilik, J. Perina, J. P. Torres, Phys. Rev. A **86**(5), 052318 (2012).

[23] P. R. Sharapova, O. V. Tikhonova, S. Lemieux, R. W. Boyd, M. V. Chekhova, Phys. Rev. A **97**(5), 053827 (2018).

[24] R. Loudon, The quantum theory of light, 3rd edition, Oxford University, 2000.

[25] S. Sensarn, G. Y. Yin, S. E. Harris, Phys. Rev. Lett. **100**(25), 253602 (2010).

[26] S. L. Braunstein, Phys. Rev. A. 71(5), 055801 (2005).

[27] W. Wasilewski, A. I. Lvovsky, K. Banaszek, C. Radzewicz, Phys. Rev. A **73**(6), 063819 (2006).

[28] M. V. Fedorov, N. I. Miklin, Contemporary Physics **55**(2), 94 (2014).

[29] A. Ekert, P. Knight, Amer. J. Phys. **63**, 415 (1995).

[30] X. Y. Li, Y. Y. Yu, B. Sun, K. P. He, J. Optoelectron. Adv. M. **17**(11-12), 1629 (2015).

*Corresponding author: linhaibo_tzvtc@163.com